35th Annual International Conference of the IEEE EMBS
Osaka, Japan, 3 - 7 July, 2013

An ADC-Free Adaptive Interface Circuit of Resistive Sensor for Electronic Nose System

Chia-Lin Chang, Shih-Wen Chiu, *Student Member*, *IEEE*, Kea-Tiong Tang, *Member*, *IEEE*

***Abstract*—The initial resistance of chemiresistive gas sensors could be affected by temperature, humidity, and background odors. In a sensing system, the traditional interface circuit always requires an ADC to convert analog signal to digital signal. In this paper, we propose an ADC-free adaptive interface circuit for a resistive gas sensor to read sensor signal and cancel the baseline drift. Furthermore, methanol was used to test the proposed interface circuit, which was connected with a FIGARO® gas sensor. This circuit was fabricated by TSMC 0.18µm CMOS process, and consumed 86.41µW under 1V supply voltage.**

I. Introduction

Olfaction is one of the human's five senses. However, many odors are not suitable for human to smell, such as poisonous and exhausted gases. In addition, humans have olfactory fatigue because of long time smelling, and olfaction differs from person to person. Nowadays, there are several researches on the electronic nose (E-nose) system. An E-nose system has various advantages including small size, low cost, low power, quantization of olfaction, the ability of long time smelling without olfactory fatigue, and the capability of being exposed to dangerous gases. Therefore, it can be applied to quality control of foods [1, 2], environmental monitoring, pollution measurement and disease diagnosis [3-5], etc.

E-nose system is a biomimetic system that mimics the mammalian olfaction, which has the ability to differentiate and classify various chemical odors. Fig. 1 shows the E-nose system and mammalian sense of smell. Gas sensor array, signal acquisition circuit and pattern recognition system in E-nose system are corresponding to olfactory cells, olfactory neurons and cerebrum in the mammalian sense of smell, respectively. Because one sensor could not detect one specific gas, a gas sensor array is required to generate a unique pattern for gas identification. There are two kinds of the conductive gas sensors, metal oxide sensor (MOS) [6,7] and conducting polymer sensor [8,9]. Metal oxide sensor has the advantages of high sensitivity (about a few ppm), long lifetime and robust, and it has been widely used. However, it has to operate at high temperature (200°C~400°C), which needs a heater and consumes large power. On the other hand, the conducting polymer sensor has the advantages of working at room temperature, high sensitivity (also about a few ppm), and its readout circuit is simple, which would be more suitable for portable devices.

Chia-Lin Chang, Shih-Wen Chiu, and Kea-Tiong Tang are with the Department of Electrical Engineering, National Tsing Hua University, Hsinchu 30013, Taiwan (e-mail: clchang@larc.ee.nthu.edu.tw; swchiu1984@gmail.com; kttang@ee.nthu.edu.tw).

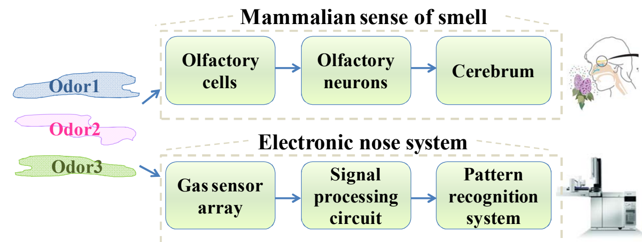

Figure 1. E-nose system and mammalian sense of olfaction.

The sensing materials of conducting polymer sensors are composed of conductive carbon black and insulating polymers, which swell reversibly and change the resistance as exposed to odors. However, the sensor resistance could be easily affected by temperature, humidity, and background odors. In addition, the resistances of each sensor in the sensor array are not the same after the deposition of different sensing materials. Therefore, an adaptive interface circuit is required to cancel the baseline drift and read the sensor signal. A number of interface circuits for resistive gas sensors have recently been proposed [10-12]. Most of them convert the sensor signal into voltage, and then deliver the voltage to an analog-to-digital converter (ADC) before further delivered to the pattern recognition system. In this paper, we propose an ADC-free adaptive interface circuit which cancels the baseline drift and converts sensor signal into digital code, so the sensor signal can be directly delivered to the digital processing stage without an ADC. Section II depicts the proposed ADC-free adaptive interface circuit connected with an integrated gas sensor in our E-nose chip. Section III shows the measurement results, and finally, Section IV provides our conclusion.

II. Architecture Description

Fig. 2 shows the structure of the proposed application-specific integrated circuit (ASIC) for the E-nose system. It contains an integrated gas sensor and an ADC-free adaptive interface circuit. We used top metal to form an interdigitated electrode of the integrated gas sensor. We could deposit the sensing material on the interdigitated electrode to form the on-chip integrated gas sensor, and it was directly connected with the adaptive interface using the remaining metal layers. Due to the integration of the gas sensor and the adaptive interface circuit on the same chip, it acheives several advantages such as small size, low cost, low power and low noise. To verify our work, we have tested one channel interface circuit connected with an integrated gas sensor. In the future, multi-channel interface circuits connected with an integrated gas sensor array will be realized to generate a unique pattern for gas identification.

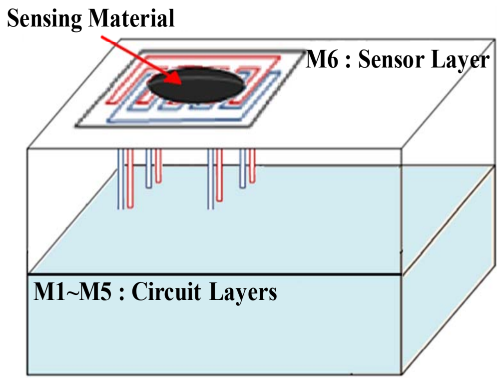

Figure 2. The structure of our E-nose chip.

A. *Integrated Gas Sensor*

Fig. 3 shows the layout of the integrated gas sensor. The top metal (Metal 6) of the TSMC 0.18μm CMOS 1P6M process was used to form the interdigitated electrodes, and the PAD mask was used to define the deposition region of the sensing material. The silicon nitride protective layer would be removed as it was defined by the PAD mask. In this way, the electrodes could directly contact with the sensing materials. Compared to a two-lead electrode structure, an interdigitated electrode structure ensured that the sensing materials uniformly distributed between the positive and negative electrodes, so they would successfully form a conductive path. The sensing area of the sensor is 250 μm × 320 μm, the width of the electrode is 16μm, and the distance between the two electrodes is 10μm.

B. *Adaptive Interface Circuit*

An adaptive interface circuit not only reads the sensor signal, but also eliminates the baseline drift caused by the temperature, humidity and background odors. Fig. 4 shows the block diagram of the proposed ADC-free adaptive interface circuit, which is composed of a comparator, an 8-bit UP/$\overline{DN}$ counter, and an 8-bit digital-to-analog converter (DAC). The output current of DAC (I_{DAC}) biases the sensor, and the magnitude of I_{DAC} is controlled by the output of UP/$\overline{DN}$ counter (D_{out}). Through the feedback loop, the ADC-free adaptive interface circuit could bias the sensor to a pre-set voltage regardless of the initial resistance of the gas sensor, and then read the sensor signal.

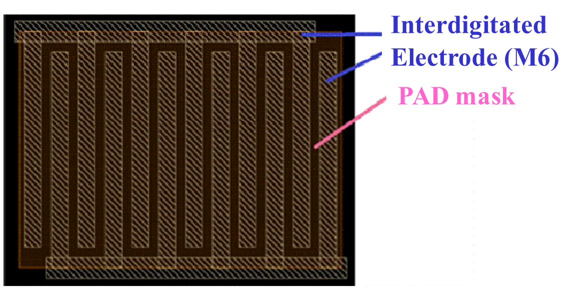

Figure 3. Layout of the integrated gas sensor. The sensing area is 250 μm × 320 μm, the width of the electrode is 16μm, and the distance between the two electrodes is 10μm.

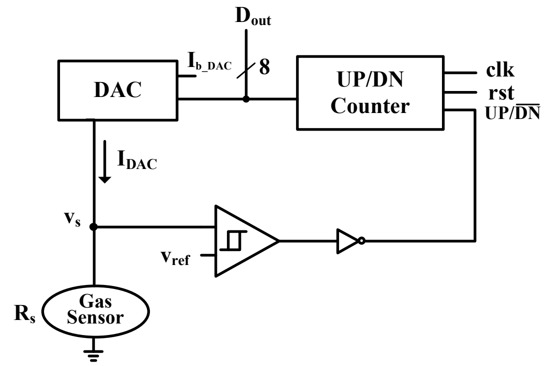

Figure 4. The block diagram of the proposed adaptive interface circuit

This circuit works in the following two mode: 1) adaptive mode: bias the sensor to a proper reference voltage V_{ref}, and 2) sensing mode: convert the sensor signal into digital code D_{out}. The operation procedures are as follows: 1) Reset the UP/$\overline{DN}$ counter to reset D_{out} to zero, the circuit is in the adaptive mode. Because the output of the comparator is low, the UP/$\overline{DN}$ counter counts up to increase I_{DAC}. 2) As the sensor voltage V_s reaches V_{ref}, the output of the comparator changes state from low to high, and then the UP/$\overline{DN}$ counter counts down. 3) As V_s is smaller than V_{ref}, the output of the comparator changes state from high to low, and then the UP/$\overline{DN}$ counter counts up again. After that, the circuit enters into sensing mode and is ready to sense gas. In sensing mode, the circuit repeats procedure 2) and 3), and V_s maintains at V_{ref} until the next reset signal.

In sensing mode, R_s changes when the gas sensor reacts with the test gas, which comes out different D_{out} to adapt I_{DAC} for maintaining V_s equal to V_{ref}. Because D_{out} is proportional to I_{DAC}, the relationship between D_{out} and R_s is shown in equation (1), where I_{b_DAC} is the unit current of DAC. Suppose R_1 is the initial sensor resistance and D_{out1} is the output of UP/$\overline{DN}$ counter at the end of the adaptive mode. In the sensing mode, the sensor resistance and the output of UP/$\overline{DN}$ counter are assumed R_2 and D_{out2}, respectively. ΔR and ΔD_{out} imply the change of resistance and the change of D_{out}, respectively. Therefore, the relationship between R_1, R_2 and ΔR is shown in equation (2), and the relationship between D_{out1}, D_{out2} and ΔD_{out} is shown in equation (3). According to equation (1) ~ (3), the percentage change of resistance $\Delta R/R_1$ can be derived as $\Delta D_{out} / D_{out\,1}$, as equation (4).

$$V_s = V_{ref} = I_{DAC} \times R_s = I_{b\_DAC} \times D_{out} \times R_s. \quad (1)$$

$$R_2 = R_1 + \Delta R. \quad (2)$$

$$D_{out2} = D_{out1} - \Delta D_{out}. \quad (3)$$

$$\Delta R/R_1 = \Delta D_{out}/D_{out2}. \quad (4)$$

In reality, the response time of gas sensor is always a few seconds. In the simulation, the response time of gas sensor was assumed only a few milliseconds, and the integrated gas sensor was replaced by a resistor. Fig. 5 shows the post-layout simulation results, where R_1=10KΩ, V_{ref}=0.7V and ΔR=10KΩ (Usually the maximum percentage change of resistance $\Delta R/R_1$ is 100%). The blue line, red line and green line correspond to Rs, Vs and D_{out}, respectively. At t=0sec, the UP/$\overline{DN}$ counter was reset, the circuit was in the adaptive mode.

At t=23.4ms, V_s reached V_{ref}=0.7V and D_{out} was 234, and then the circuit entered into the sensing mode. At t=30ms, suppose the gas sensor was exposed to an odor. The sensor resistance started increasing, and the counter also started counting down to decrease I_{DAC} for keeping $V_s=V_{ref}$. At t=65ms, the sensor resistance saturated to 20KΩ, and D_{out} was 117. At t=70ms, the odor was flushed out. The sensor resistance started decreasing and the counter also started counting up for keeping $V_s=V_{ref}$.

According to the above simulation results, Fig. 6 shows that $\Delta D_{out}/D_{out2}$ is proportional to $\Delta R/R_1$. Consequently, R_s could be obtained from D_{out}, and equation (4) depicts the relationship between R_s and D_{out}. By this adaptive interface circuit, D_{out} could be directly delivered to the digital signal processing stage without an ADC, reducing the chip area, complexity and power consumption of the E-nose system. The adaptive interface circuit was fabricated by TSMC 0.18μm CMOS process and operated under 1V supply voltage. Fig. 7 shows the chip photo, and the integrated gas sensor was on the top of the adaptive interface circuit.

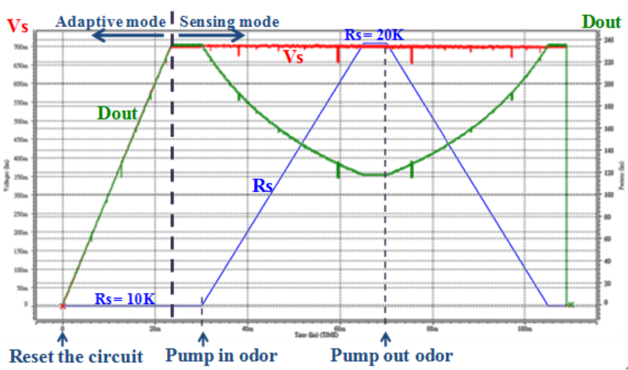

Figure 5. Post-layout simulation when initial resistance of gas sensor R_1=10KΩ , V_{ref}=0.7V and ΔR=10KΩ.

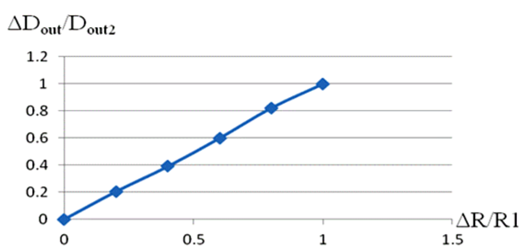

Figure 6. $\Delta D_{out}/D_{out2}$ versus ΔR/R1 according to the simulation result as Rs reacts from 10KΩ to 20KΩ

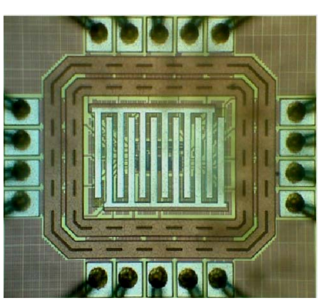

Figure 7. The chip photo of the integrated gas sensor and the proposed adaptive interface circuit.

III. Measurement Result

Before depositing the sensing material, the two electrodes were open, so the gas sensor (Rs) could be directly replaced by an off-chip resistor. Fig. 8 shows the measurement results of D_{out} versus R_s as V_{ref} = 650mV and the bias current of DAC I_{b_DAC} =1μA, where R_s was replaced by a variable resistor varying from 2.5KΩ to 80KΩ. Fig. 9 shows the measurement results of D_{out} versus R_s as V_{ref} = 700mV and the bias current of DAC I_{b_DAC} =330nA, where variable resistor R_s varied from 10KΩ to 165KΩ. Table 1 shows the summary of the chip specification.

For gas experiments, the adaptive interface circuit was connected with a commercial FIGARO® TGS-2610 gas sensor to replace the integrated gas sensor. FIGARO® TGS-2610 gas sensor is a metal oxide gas sensor, and the sensor resistance reduces when it is exposed to odors, opposite to the conducting polymer gas sensor. However, the same relationship between D_{out} and R_s could be derived.

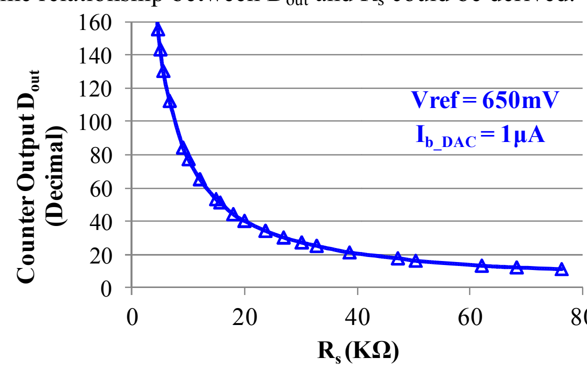

Figure 8. Measurement results of D_{out} versus R_s at V_{ref} = 650mV and R_s varied from 2.5KΩ to 80KΩ

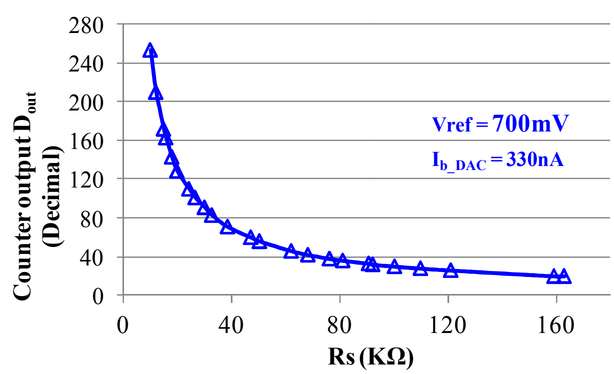

Figure 9. Measurement results of D_{out} versus R_s at V_{ref} = 700mV and R_s varied from 10KΩ to 165KΩ

TABLE I. Chip Specifications

Specification	Measurement Result
Process	TSMC 0.18μm CMOS 1P6M
Power Supply	1V
Power Dissipation	86.41μW
Adaptive resistance range	10KΩ~500KΩ
Chip size (mm^2)	0.72623 x 0.6541

Fig. 10 shows the setup and the experimental steps. A FIGARO® TGS-2610 gas sensor was placed into a 4-neck bottle chamber, and a motor was used to flush the chamber. The condition of the interface circuit was set to be the same to the chip measurement in Fig. 8. Fig. 11 shows the gas experimental results of D_{out} and $\Delta D_{out}/D_{out2}(=\Delta R/R_1)$. At t=0sec, the UP/$\overline{DN}$ counter was reset and the circuit was in the adaptive mode. In 0~20 sec, Vs tracked to V_{ref}, and then the circuit entered into sensing mode. At t=20 sec, 3ul methanol was injected into the 4-neck bottle chamber. In 20~230 sec, the sensor was exposed to methanol vapor, and the sensor resistance decreased and D_{out} increased. At t=230 sec, the gas was flushed out, the sensor resistance increased and D_{out} decreased. Another reset signal should be given before next gas experiment. According to the above experiment results, R_s could be obtained from equation (4) and Fig. 8. Consequently, the ADC-free adaptive interface circuit worked successfully as expected. In the future, we plan to deposit proper sensing materials on the interdigitated electrodes, and then realize the same gas experiment..

IV. CONCLUSION

We proposed an ADC-free adaptive interface circuit which V_s could automatically track to V_{ref} and cancel the baseline drift. The sensor signal was converted into digital code, so it could be directly delivered to the digital processing stage of recognition system without an ADC, which was area efficient. The percentage change of resistance $\Delta R_s/R_1$ could be obtained from $\Delta D_{out}/D_{out2}$. For circuit verification, the adaptive interface circuit has been connected with a metal oxide gas sensor, FIGARO® TGS-2610, and the gas experiment has been executed with methanol vapor. The chip test and gas experiment showed the ability to cancel baseline drift and readout the gas sensor with low power (86.41µW). The circuit was fabricated by TSMC 0.18µm process and operated under 1V supply voltage, which is suitable for a portable E-nose system. In the future, sensing materials will be deposited on the interdigitated electrode to form the on-chip integrated gas sensors, and multi-channel interface circuit for a sensor array and microcontroller will be integrated on the same chip to implement the E-nose SoC.

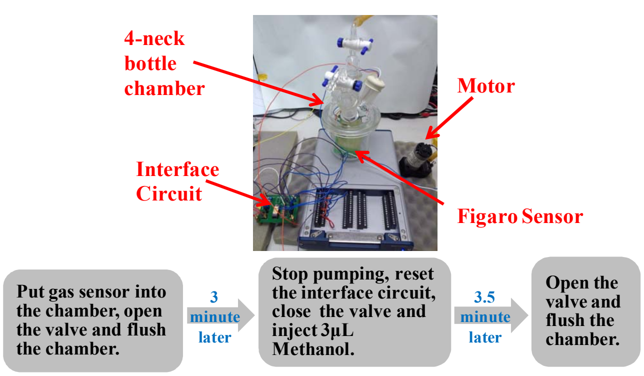

Figure 10. The gas experiment environment and the experiment steps.

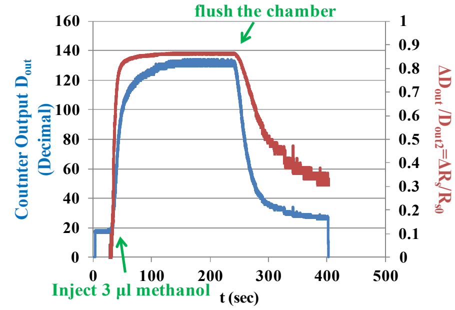

Figure 11. The gas experiment result of D_{out}, $\Delta D_{out}/D_{out2}$ and $\Delta R/R_1$.

ACKNOWLEDGMENT

The authors would like to thank financial support of the National Science Council of Taiwan, under Contract NSC 101-2220-E-007-006. The authors would like to acknowledge the support of National Chip Implementation Center (CIC), Taiwan for chip fabrication.

REFERENCES

[1] B. Tudu, A. Metla, B. Das, N. Bhattacharyya, A. Jana, D. Ghosh, and D. Bandyopadhyay, “Towards versatile electronic nose pattern classifier for black tea quality evaluation: An incremental fuzzy approach,” IEEE Trans. Instrum. Meas., vol. 58, no. 9, pp. 3069–3078, Sep. 2009.

[2] I. Concina, M. Falasconi, and V. Sberveglieri, “Electronic Noses as Flexible Tools to Assess Food Quality and Safety: Should We Trust Them?, ” Sensors Journal, IEEE, vol. 12, pp. 3232-3237, 2012.

[3] G. Dongmin, D. Zhang, L. Naimin, D. Zhang, and Y. Jianhua, “A Novel Breath Analysis System Based on Electronic Olfaction,” Biomedical Engineering, IEEE Transactions on, vol. 57, pp. 2753-2763, 2010.

[4] A. D’Amico, C. Di Natale, R. Paolesse, A. Macagnano, E. Martinelli, G. Pennazza, M. Santonico, M. Bernabei, C. Roscioni, G. Galluccio, R. Bono, E. Finazzi Agrò, and S. Rullo, “Olfactory systems for medical applications,” Sen. Actuators B, Chem., vol. 130, pp. 458–465, 2008.

[5] A. H. Abdullah, A. H. Adom, A. Y. M. Shakaff, M. N. Ahmad, A. Zakaria, F. S. A. Saad, et al., “Hand-Held Electronic Nose Sensor Selection System for Basal Stamp Rot (BSR) Disease Detection, ” in Intelligent Systems, Modelling and Simulation (ISMS), 2012 Third International Conference on, 2012, pp. 737-742.

[6] I. Kiselev, M. Sommer, J. K. Mann, and V. V. Sysoev, “Employment of Electric Potential to Build a Gas-Selective Response of Metal Oxide Gas Sensor Array,” Sensors Journal, IEEE, vol. 10, pp. 849-855, 2010.

[7] N. Kwan Ting, F. Boussaid, and A. Bermak, “A CMOS Single-Chip Gas Recognition Circuit for Metal Oxide Gas Sensor Arrays,” Circuits and Systems I: Regular Papers, IEEE Transactions on, vol. 58, pp. 1569-1580, 2011.

[8] S. M. Briglin, M. S. Freund, B. C. Sisk, and N. S. Lewis, “Vapor detection, classification, and quantification performance using arrays of conducting polymer composite chemically sensitive resistors,” in Sensors, 2002. Proceedings of IEEE, 2002, pp. 727-731 vol.1.

[9] A. S. Haynes and P. I. Gouma, “Electrospun Conducting Polymer-Based Sensors for Advanced Pathogen Detection, ” Sensors Journal, IEEE, vol. 8, pp. 701-705, 2008.

[10] M. Grassi, P. Malcovati, and A. Baschirotto, "Flexible high-accuracy wide-range gas sensor interface for portable environmental nosing purpose," in Circuits and Systems, 2005. ISCAS 2005. IEEE International Symposium on, 2005, pp. 5385-5388 Vol. 6.

[11] T. J. Koickal, A. Hamilton, S. L. Tan, J. Covington, J. W. Gardner, and T. Pearce, "Smart Interface Circuit to Ameliorate Loss of Measurement Range in Chemical Microsensor Arrays," in Instrumentation and Measurement Technology Conference, 2005. IMTC 2005. Proceedings of the IEEE, 2005, pp. 548-550.

[12] X. Mu, E. Covington, D. Rairigh, C. Kurdak, E. Zellers, and A. J. Mason, "CMOS Monolithic Nanoparticle-Coated Chemiresistor Array for Micro-Scale Gas Chromatography," Sensors Journal, IEEE, vol. 12, pp. 2444-2452, 2012.